12-17-2020

On the Effective Finite Element Simplification of Bolted Joints: Static and Modal Analyses

Abdulrahman Mohammad Ibrahim
axi3505@rit.edu

RIT

On the Effective Finite Element Simplification of Bolted Joints: Static and Modal Analyses

By

Abdulrahman Mohammad Ibrahim

A Graduate Capstone project Submitted in Partial Fulfilment of the Requirements for the Degree of Master of Engineering in Mechanical engineering

Department of Engineering

KATE GLEASON COLLEGE OF ENGINEERING

Rochester Institute of Technology

RIT Dubai

December 17, 2020

RIT

Master of Engineering in

Mechanical engineering

Graduate Paper/Capstone Approval

Student Name: Abdulrahman Mohammad Ibrahim

Capstone Title: On the Effective Finite Element Simplification of Bolted Joints: Static and Modal Analyses

Graduate Capstone Committee:

Name: Prof. Wael Abdel Samad Designation: Chair of committee Date :

Type of the Paper (Article)

On the Effective Finite Element Simplification of Bolted Joints: Static and Modal Analyses

Abdulrahman M. Ibrahim[1] and Wael A. Samad[2,*]

[1] Rochester Institute of Technology – Dubai; Graduate Student - Mechanical Engineering; aaxi3505@g.rit.edu
[2] Rochester Institute of Technology – Dubai; Associate Professor - Mechanical Engineering; wascad@rit.edu
* Correspondence: wascad@rit.edu; Tel.: +97143712081

Abstract: In this paper, the finite element simplification of a standard bolted joint configuration is investigated. Static and modal analyses of a 3D model are used for benchmarking three different simplified finite element models using Siemens NX software. More specifically, the three simplified finite element models utilize beam elements, spring elements and a coupled shell-beam-spring elements model. Four margin of safety criteria with respect to slipping, gapping, yield strength and ultimate strength were evaluated. Results show comparable values in the yield and ultimate margins of safety of all three simplified finite element models. Additionally, a parametric analysis relative to bolt size is performed to check the validity of the different simplifications with respect to bolt slenderness ratio. Results indicate minimal errors for larger slenderness ratio bolts. This is attributed to the minimal contribution of shear and out of plane stresses. For optimal results, it is recommended for the slenderness ratio to be at least 1.5 for an accurate 1D representation of the overall join behavior. Moreover, all three simplifies models are observed to accurately capture modal frequencies, with the exception of the torsional modes due to restricted degrees of freedom. Finally, effects of beam discretization and computational time is highlighted in the work presented in this manuscript.

Keywords: Bolted joint, FEM, simplification methods, 3D elements, 1D elements, beam elements, spring elements, margin of safety, modal analysis

1. Introduction

Bolted joints are commonly used mechanical fasteners to connect separate mechanical or structural members together [1,2]. Bolted joints are considered to be one of the most essential mechanisms in the aerospace industry, among other removable mechanical joints, such as pinned or riveted joints [3]. Bolted joints have better tensile strength and fatigue life compared to pinned, welded, or riveted joints [4-6], and hence their wide usage. Knowing the importance and vast range of applications of bolted connections, it is crucial for structural engineers to accurately and efficiently calculate and analyze the slipping, gapping and yield margins of safety as well as other mechanical characteristics to have a more confidant design and bolt sizing. In fact, a bolted member's structural response depends heavily on bolt-hole clearance [7]. Although field-assembled bolted joints frequently possess a reasonable amount of bolt-hole clearance [8] and aerospace connections are often snug-fitting [9]. Reference [10] demonstrates the severe stress consequences due to clearance in bolted aluminum structures; this is especially important fatigue-wise when systems are exposed to cyclic loading.

Several analytical approaches can be used to calculate and predict the resultant deformations, stresses, natural frequencies, etc. However, with the increasing complexity of new designs, the analytical approach can only be relied on to produce conservative estimates of the oversimplified models where assumptions are applied in many aspects. For example, in the case of orthotropic materials or composites, testing has to be performed on those materials to find their mechanical behavior to obtain results using the classical analytical approach. Moreover, the analysis of such assemblies is highly dependent on

loading and boundary condition, making it difficult for an accurate analytical approach to be meaningfully applied.

Moreover, and while experimental methods, such as digital image correlation (DIC) and thermoelastic stress analysis (TSA), have the ability to provide actual full-field displacement, strain and/or stress data in loaded bolted connections, they require a good amount of post processing to extract meaning information related to strength criteria and bolt sizing. For instance, DIC can provide accurate 2D displacement fields on the surface of the bolted connection. Such displacement will then need to be mathematically differentiated (often using Lagrangian formulation) to arrive at strains. Moving from strains to stresses will of course then require Hooke's law and the necessary accompanying material properties (Young's modulus and Poisson's ratio). Therefore, and while DIC data can be useful if full-field displacement field is the objective, plenty of limitations and loss of information will be incurred when measured displacements are converted to stresses for strength criteria. It is worth mentioning that DIC data can be coupled with analytical formulations in certain loading and geometry scenarios. [11]. Moreover, such experimental techniques will have limitations in their ability to replicate different loading scenarios in a laboratory setting.

With all the drawbacks of analytical and experimental approaches summarized, finite element methods (FEM) has an obvious advantage in analyzing and modeling bolted joints. It is considered the most efficient method of modeling and analyzing complex structures [12], such as one with multiple joints and complex shapes. Using FEM, solutions can be obtained for all problems, while boundary conditions, loads, material properties can be incorporated into the model more accurately with more details. This is achieved by dividing the studied part into small elements/nodes where the software can calculate for the unknown value at each node. The values are interpolated to find the results in the elements connecting the nods. Therefore, it can be seen how increased model complexity impacts the computational cost and result accuracy. Engineers need to effectively simplify their analysis to save computational time without compromising on the results accuracy [13-16]. Another thing that should be taken into account when using FEM is model convergence. This is an iterative stage where model convergence is achieved when the results/results accuracy are no longer affected by further reducing the mesh density.

The joint's two primary characteristics that need to be considered when analyzing bolted joints are the joints' preload and the mating contact area [17]. This can be modeled using many modeling techniques, such as single elements or a combination of solid elements, spider 1D elements, contact boundary conditions, and applied forces [18]. Keeping in mind that with every added complexity, the computational cost increases significantly while leaving more room for unpredictable error and uncertainty [19].

Moreover, and while not deviating from the current focus of this paper, the study of simplification and reductions in finite element models is not restricted to structural mechanics (e.g. bolted joins). The biomedical field is a main driver in this area due to the level of complexity their finite element models entail. Such complexity necessitates cutting down on computational and processing time by performing model simplifications and dimensional reduction techniques to finite element models [20]. Examples of such applications are in the design and optimization of dental implants [21] and [22] as well as stress analysis of prosthetics [23].

1.1. Bolt/fasteners masses

In most cases, the fasteners' mass is relatively small compared to the overall structure assembly, making the bolt's mass effect negligible [24]. This allows for more flexibility in modeling the bolts using simplified finite element models without loss of information.

1.2 Yield and ultimate strength

The yield strength and ultimate strength for both the bolt and the mounting plates are crucial when performing structural analysis on the whole assembly. Coupling to parts together generates stress concentration near the coupled areas within the bolt itself. Finite element analysis can help identify these hidden localized stresses and identify possible failure points to optimize the design accordingly.

1.3 Stiffness

The type of coupling between two components in a structure can affect the stiffness of the system. Different modeling techniques can affect the structures' natural frequency when performing modal analysis [13, 25]. This relation between stiffness, natural frequency, and coupling conditions can be used to compare and validate analysis results and testing results. Another advantage of FE analysis with regards to natural frequencies is the ability to study some of the more complex torsional modal shapes of a structure. However, research has shown that in some cases, especially in dynamic analysis of simplified models, model tuning is required to account for the simplified geometries, such as damping coefficients, non-structural masses, etc.

1.4 Slipping and gapping

Slipping in bolted joints is one of the most commonly easy to neglect phenomenon in the design of steel structures, while it is also one of the most crucial elements to be considered in the system [26]. Slippage in bolted joints could result in shear failure of the joint regardless of the joint capacity due to the deformation associated with the introduced lateral shear [26, 27]. Bolted joints are preloaded to prevent gapping and increase the system's stiffness [27, 28]. Gapping occurs when the contact surfaces of the bolts/washers are separated from the mounting area. This is often due to bolt or component deformation due to high loads.

1.5 Thread engagement depth

For metal and steel components, it is recommended to have a minimum thread engagement to be 1.5 of the diameter (1.5D) of the bolt to ensure that optimum joint strength [28-30].

1.6 Computational cost and accuracy

Designing a new concept is a very iterative process to satisfy all the required characteristics in the optimum configuration, such as mass, volume, and other mechanical factors. This is why it is vital to have an efficient computational approach to study and revise the design faster and more effectively. For example, increasing the mesh size density can improve the overall accuracy of the analysis, while on the downside, it can also increase the computational cost significantly [32, 12]. The same goes for raising the model's complexity and using 3D elements that incorporate all the system's small details.

1.7 Margin of safety

Simplified margin of safety (MoS) for bolts slipping, gapping, ultimate strength and yield strength based on (ECSS-E-HB-32-23A) [33, 34]. For slipping and gapping:

$$MoS_{slip} = \frac{P_{o(min)} \times \mu}{S.F. \times F_{lateral}} - 1 \quad (1)$$

$$MoS_{gap} = \frac{P_{o(min)}}{S.F. \times F_{axial}} - 1 \quad (2)$$

Where μ is the friction coefficient (set to 0.3), $P_{o(min)}$ is the minimum imbedded preload, F_{axial} is the axial load applied to the bolt and $F_{lateral}$ is the lateral load applied to the bolt. For ultimate and yield strength:

$$MoS = \frac{allowable\ Load}{external\ \ load \times SF} - 1 \quad (3)$$

For yield failure criteria and ultimate failure criteria respectively:

$$MoS_y = \frac{A_s \sigma_y}{F_A SF_y} - 1 \quad (4)$$

$$MoS_{ult} = \frac{A_s \sigma_{ult}}{F_A SF_{ult}} - 1 \quad (5)$$

Where $SF_y = 1.25$ and $SF_{ult} = 2.0$ are used for the two criteria respectively. These values used are based on general practices and standards relevant to the aerospace industry, where bolts and mechanical fasternes are prevalant. the case of untested structures, yield factor of safety is taken as 1.25 and the ultimate factor of safety is taken as 2.0 [35, 36]. Because all safety factors are incorporated into all appropriate equations, the MoS only needs to be a positive value for the bolt to meet the requirement. This margin was used as one of the benchmarking tools to compare the simplified finite element models against the full 3D one.

2. Methodology

2.1. Software

The CAD (computer-aided design) and CAE (computer-aided engineering) platforms used in this study are NX Nastran. A single M5 bolt is used in a bolted joint scenario referred to as joint #13 as per the ECSS handbook [33]. The CAD model and finite element model are solved using linear static analysis (referred to as SOL 101 in NX Nastran software) and using real eigenvalues modal analysis (referred to SOL 103 in NX Nastran software). The models are solved for each specific case under three sub-cased loading scenarios $\boldsymbol{F_x}$, $\boldsymbol{F_y}$ and $\boldsymbol{F_z}$. A full 3D finite element model, referred to throughout this manuscript as case-1, is used to benchmark both static and modal results of the dimensionally reduced finite element under investigation in this manuscript.

2.2. Bolt Specifications

For this study, M5 Bossard A2-70 stainless steel bolt was used, having the following properties and dimensions listed in Table 1 [37].

Table 1. Bolt Specifications

Bolt Data	Value	Unit
Nominal Diameter	5	mm
Thread pitch, p	0.8	mm
The nominal friction coefficient in thread -bolt head, $\mu_{threads}$	0.3	
Bolt friction uncertainty	0.1	
Pitch Diameter, d_{pitch}	4.48	mm
Effective Contact diameter (Collar Diameter), d_c	10	mm
Bolt stress area, A_r	14.18	mm^2
Alpha, α	30	deg.

Based on ECSS standards [32, 33], the bolt preload is calculated as follows:

$$P_{o(min)} = \frac{T}{K\ d_b} \times 0.95 \quad (6)$$

Where $\boldsymbol{P_{o(min)}}$ is the minimum imbedded initial bolt preload (MPa) (-5% imbedding), $\boldsymbol{T}$ is the nominal tightening torque specified from the manufacturer [29], $\boldsymbol{d_b}$ is the bolt nominal diameter and $\boldsymbol{K}$ is the nut factor evaluated using Equation (7) below:

$$K = \frac{d_{bolt}}{d_{pitch}}\left(p + \frac{\pi \mu_{threads} \times d_{pitch}}{coscos\ (\alpha)}\right)\left(\pi\ d_{pitch} - \frac{\mu_{threads} \times p}{coscos\ (\alpha)}\right) + 0.625\ \mu_{threads} \quad (7)$$

3. Modeling

3.1. CAD

The CAD model used in the study is shown in the annotated Figure 1. The top plate has a 5.5 mm clearance hole and a 10 mm diameter circle representing the bolt/washer effective contact area. The bottom fixing plate has a 5 mm tapped hole and the effective thread engagement is 7.5 mm through the depth of the hole (1.5D) [29-31].

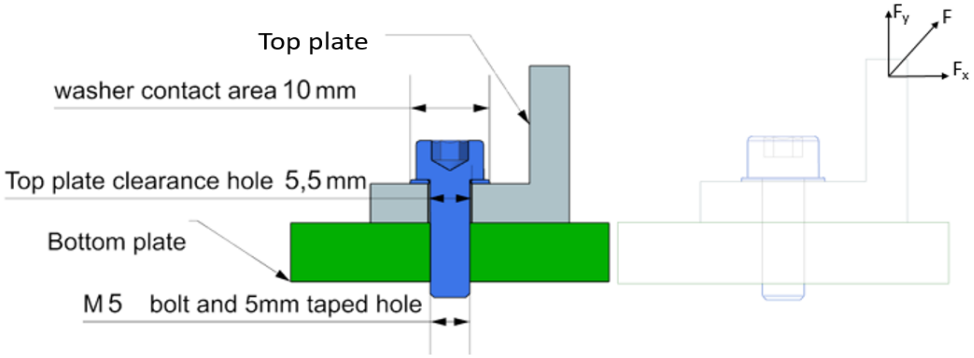

Figure 1. Solid and wireframe view of the bolt CAD model

3.2. Material Properties

The material properties used for the bolt and the mounting plates of the model are listed in Table 2.

Table 2. Model material properties

Bolt - Bossard A2-70		
Bolt yield strength	450	MPa
Bolt ultimate strength	700	MPa
Modulus of elasticity	193	GPa
Poisson's ratio	0.34	
Density	8 x 10^{-6}	kg/mm^3

Top and bottom mounting plates - AL6061		
Plate yield strength	276	MPa
Plate ultimate strength	310	MPa
Modulus of elasticity	69	GPa
Poisson's ratio	0.33	
Density	2.711 x 10^{-6}	kg/mm^3

3.3. Finite Element Models

As mentioned earlier, this manuscript compared three simplified finite element models with respect to a full 3D one. The full 3D one is referred to as case-1 and is used for benchmarking both modal and static analysis results. The three simplified finite element models are referred to as case-2, case-3 and case-4. All cases are elaborated on in the proceeding subsections.

3.3.1 Case-1 (Detailed 3D model)

This finite element model was created using 3D-swept and 3D-tetrahedral elements. The 3D-tetrahedral elements were used to model the bolt with a fine mesh density, incorporating all detailed features of the bolts' curved surfaces. The bottom fixing plate is clamped at both ends in the Y-axis. Spider RBE2 element is used at the top of the top plate to simulate the applied force by applying it at the spider connection's top node. This assumes that the applied load is fully clamped to the top face of the applied area. The bolts' head is clamped to the top plate using the effective contact area shown in Figure 1**Error! Reference source not found.**. The thread engagement is then simulated using a surface glue boundary condition to clamp the bolts' thread with the bottom fixing plate, as shown in Figure 2. Note that the contact between the bolt and the clearance hole is not defined in the model, since the is a 0.5 mm clearance gap. This is deemed acceptable as the shear deformation effect between the bolt body and the clearance hole would only show if we were running dynamic nonlinear analysis in the case of slipping. Moreover, the bolt head has a surface contact with 0.3 friction coefficient and imbedded preload based on the bolt size. In the case of the M5 bolt, the minimum imbedded preload is set to 2,143 N, while the engaged threads have a surface-to-surface glue contact. Glue creates stiff springs or a weld like connection to prevent relative motion in all directions. Finally, in this 3D model the surface contact was defined as "no penetration" and a friction coefficient of 0.3.

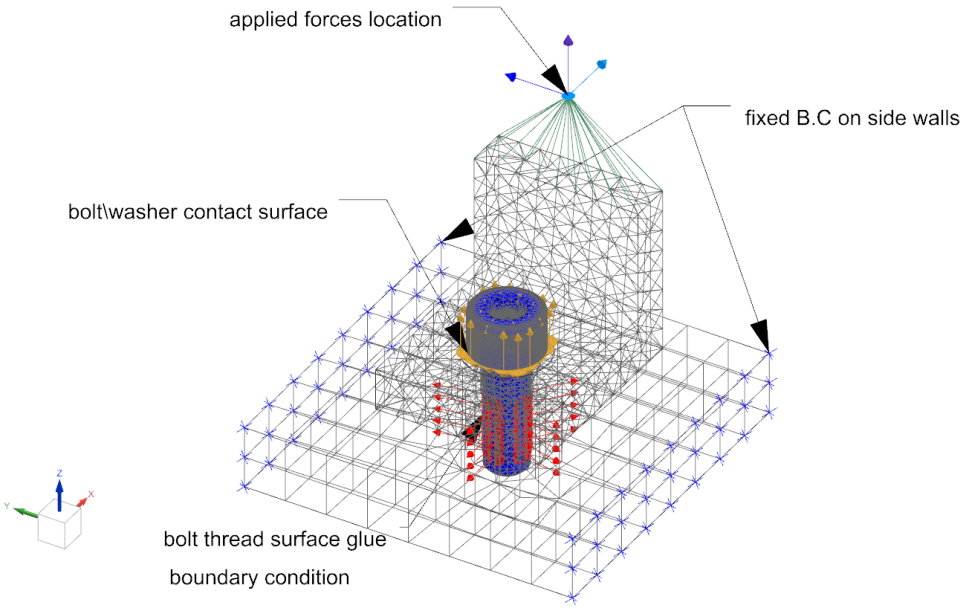

Figure 2. 3D FE model constraints and boundary conditions (case-1)

3.3.2 Case-2 (RBE2 - Simplified FE model)

In this first simplified model, solid 3D elements were replaced with planer 2D shell elements. Connections and coupling between the parts were made using 1D elements. A combination of rigid body elements (RBE2/RBE3), beam elements, and spring elements,

Figure 3. As shown in Figure 4, the "2" in the (RBE2) stands for the type of joint the 1D connection has with respect to the end nodes. All the nodes in an RBE2 connection are considered rigidly connected (Siemens, CAE-1D connection). Therefore, local rotation is not imposed at the edge nodes (Nastran Elements Guide). For the case of RBE3 1D element, local rotation about the end nodes is allowed, permitting the load to be evenly distributed without having a fully coupled rigid connection. In this study, RBE2 simulated the rigid connection of the bolts' engaged threads to the fixed bottom plate. Simultaneously, RBE3 elements were used to simulate the clamping between the bolts' head and the top plate in compliance with the effective bolt contact area.

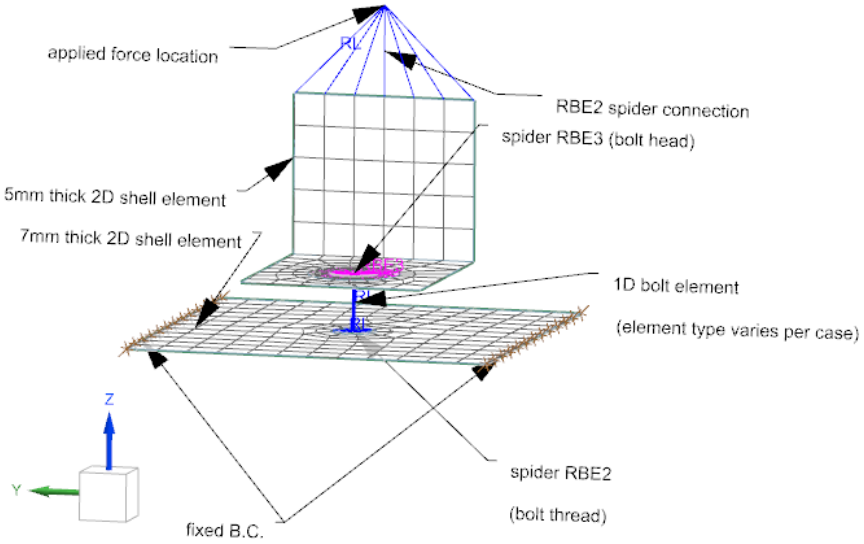

Figure 3. Simplified FE model using 1D elements and 2D-shell elements (case-2)

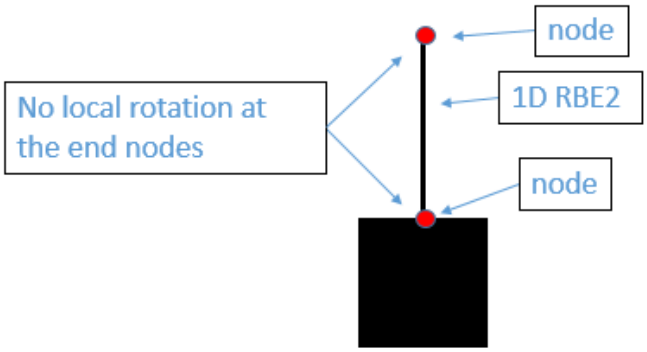

Figure 4. Rigid body element (RBE2)

Similar to the 3D FE model, the simplified model is based on the same CAD model, where 2D shell elements are used at the mid surface of the plates, and a combination of 1D and spider 1D elements are used to represent the bolt and bolt clamped areas, Figure 3. The bolt-effective contact area (bolt head) with the top plate is generated using spider RBE3 connection. RBE3 allows having an evenly distributed load that represents the connection without significantly affecting the overall stiffness. The thread engagement area is a more rigid coupled connection; hence RBE2 is used to simulate the thread connection to the bottom plate. The bolt is simulated using a single 1D element that connects the two central nodes of the top and bottom spider connections. RBE2 1D connection is used in case-2 to simulate the 1D bolt element.

3.3.3 Case-3 (Beam - Simplified FE model)

In this second simplified finite element model, the bolt is dimensionally reduced to a beam element with a rod cross-section of 5mm diameter and stainless steel material properties, Figure 5. Compared to the rigid element in case-2, the 1-D beam allows for element expansion, tension and bending in two perpendicular planes, which reduces the risk of increasing the overall stiffness of the system. It also incorporates the torsional stiffening effects of the bolt and the shear stresses within the bolt element making it a more realistic frequency dependent 1-D bolt.

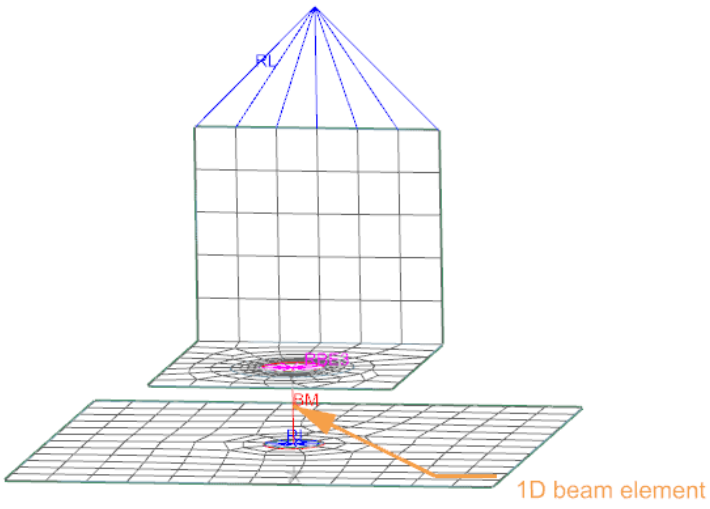

Figure 5. 1D beam element representation (case-3)

3.3.4 Case-4 (spring - simplified FE model)

In this fourth and last simplified finite element mode, the 1D bolt is modeled using a spring element with a very high stiffness value, Figure 6. Similar to the beam element in case-3, the spring element can simulate a frequency dependent 1D bolt using a generalized spring/damper element to represent the bolt clamping characteristics. It also allows defining the stiffness values along multiple DOF, however, the stiffness values for all DOF are assumed to be uniform for this case study.

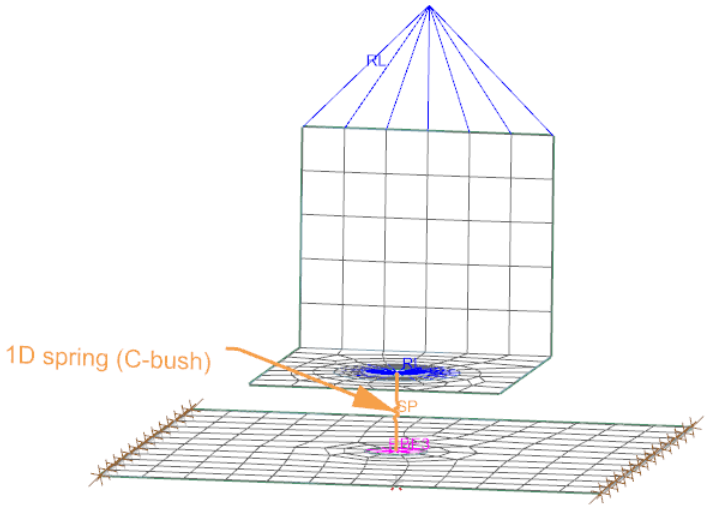

Figure 6. 1D spring element representation (case-4)

3.3.5 Summary of all cases

Now that all the 4 cases have been introduced, Table X below serves as a detailed summary for all the finite element models used in this manuscript.

Table 3. Summary for all 4 NX finite element models used

Case	*Element type*	*Sub type (NX terminology)*	*Targeted element size*	*Location*	*Notes*
1	*3D solid swept mesh*	*CHEXA(8)*	*1.5 mm*	*Bottom plate*	*8 nodes* 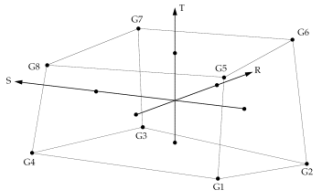
	3D solid tetrahedral mesh	*CTETRA(4)*	*1.5 mm*	*Top plate*	
	3D solid tetrahedral mesh	*CTETRA(4)*	*1.5 mm*	*Bolt*	*Surface curvature-based size variation was activated to allow the mesh to capture all geometrical aspects of the bolt*
2,3,4	*2D mesh*	*CQUAD4*	*3.25 mm*	*Bottom plate*	*Mid-plane, 7 mm thickness*
	2D mesh	*CQUAD4*	*3.23 mm*	*Top plate*	*Mid-plane, 5 mm thickness*
2	*1D beam rigid body element*	*RBE2*	*1 element*	*Bolt*	
3	*1D beam (CBEAM)*	*PBEAML – rod cross section*	*1 element*	*Bolt*	*5mm ROD cross section for M5 bolt*
4	*1D spring element*	*Cbush*	*1 element*	*Bolt*	*Defines a generalized spring-and-damper structural element that may be nonlinear or frequency dependent.*

3.4. Solution Setup

It is assuming that the bottom plate is clamped at the Y-direction sides. A force of 50N was applied in X, Y, and Z- directions as three separate sub-cases in the solution, Figure 7.

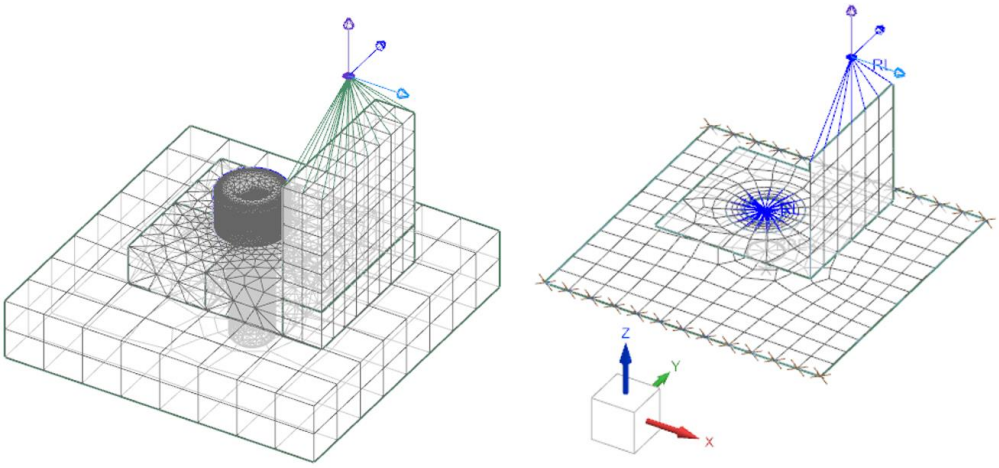

Figure 7. Applied loads on detailed model of case-1 (left) and simplified model (right)

4. Results

4.1. Convergance analysis

Prior to comparing the different simplified finite element models of cases -2, -3 and -4, a convergence study was performed to determine the minimum number of 3D elements. This is essential so that the different simplified models can compared against near exact results. The convergence analysis was performed for the case where a static load of $\boldsymbol{F_x = 50\ N}$ was applied to the upper plate as shown in Figure 2. The mesh density was varied and the model solved while recording the number of elements and the corresponding maximum Von Mises stresses for each. The 3D model was deemed satisfactory and predicting near exact results when the percentage difference between two subsequent 3D models was below 1%. The results of the convergence analysis are presented in Table 4. The 6th iteration which utilized 114,340 elements its model was the one used for benchmarking the three simplified finite element models of case-2, case-3 and case-4.

Table 4. 3D model convergence analysis

Satic loading scenario, F_x		
# of elements	**Maximum Von Mises stresses (MPa)**	**percentage difference**
81,201	154.8	NA
81,646	150.6	2.7%
82,549	147.3	2.2%
87.764	143.75	2.4%
104,105	140.5	2.3%
114,340	141	0.4%
128,514	141.3	0.2%
133610	141.8	0.4%

4.2. System stiffness evaluation (modal)

The systems' stiffness is compared by solving for the modal responses, then comparing the natural frequencies in each case. Real-eigenvalues solution (SOL 101) is used to compute the values for the four cases being investigated. Figure 10 shows the first ten

modal responses obtained from the analysis. The response analysis shows that case-3 had a similar stiffness response to case-1. While case-2 and case-3 show that the increased rigidity that is assumed for the RBE2 elements and spring elements overestimate the system's overall stiffness.

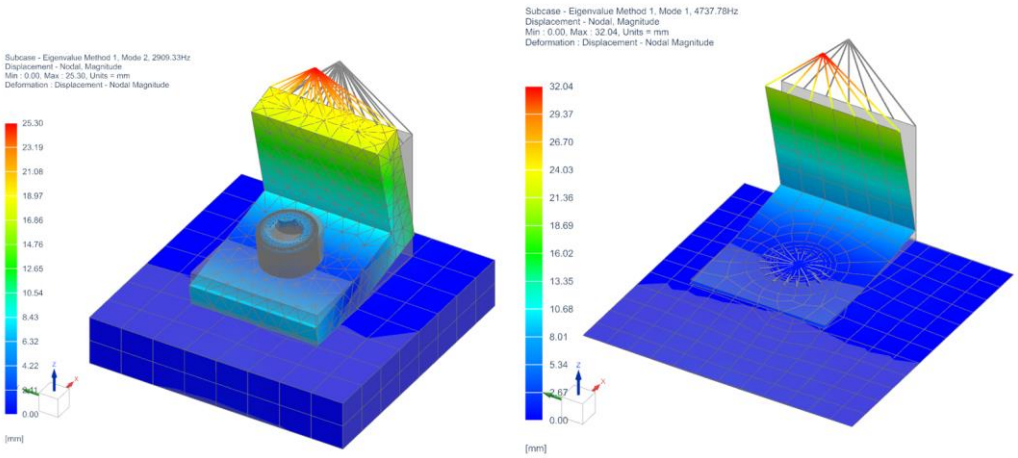

Figure 8. 2nd mode nodal deformation for case-1 (left) and case-2 (right)

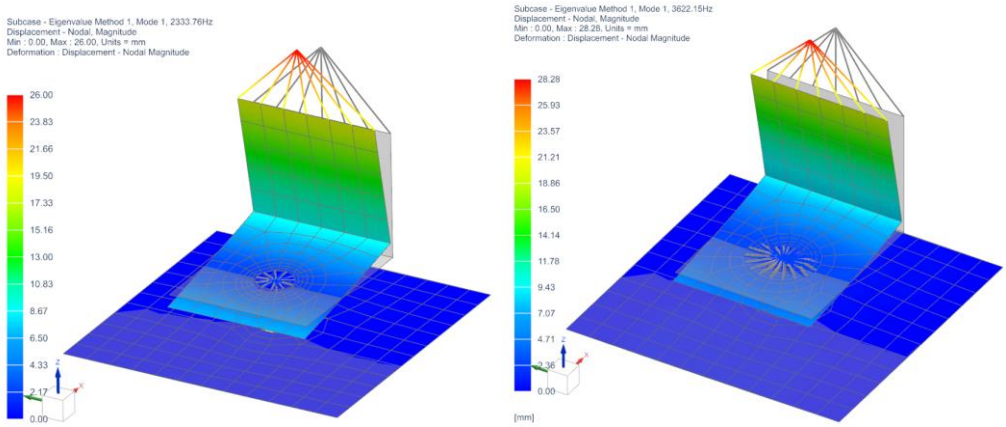

Figure 9. 2nd mode nodal deformation for case-3 (left) and case-4 (right)

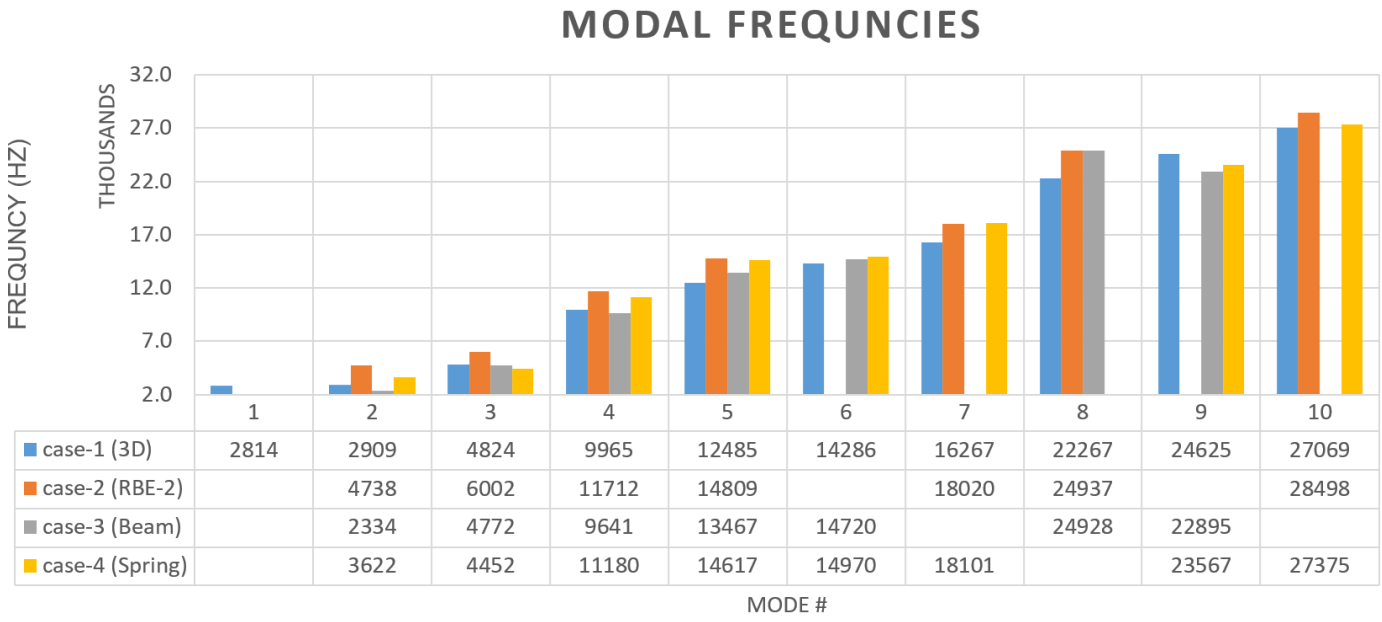

Figure 10. Modal frequency summary for all 4 cases

It was also noticed that at extremely high-frequency values (modes 10, 11, and 13), case-2 and case-4 seem to estimate better the modal frequency having closer value to the detailed model in case-1 as the summary of the results tabulated in Table 5 show.

Table 5. Percentage difference in mode shapes of the cases-2, 3 and 4 with respect to case-1

mode	case-1 (Hz)	case-2 (%)	case-3 (%)	case-4 (%)
1	2814	-	-	-
2	2909	63%	20%	25%
3	4824	24%	1%	8%
4	9965	18%	3%	12%
5	12485	19%	8%	17%
6	14286	-	3%	5%
7	16267	11%	-	11%
8	22267	12%	12%	-
9	24625	-	7%	4%
10	27069	5%	-	1%
11	33051	4%	-	1%
12	35366	-	-	-
13	36937	5%	1%	1%

Looking into mode 1 and mode 12, which where only captured in the detailed 3D model (Figure 11**Error! Reference source not found.** & Figure 12). It is notice that these two modes are local torsional modes that are dependent on the ability of the 3D model to show rotational and torsional degrees of freedom. These modes were not captured in the

any of the simplified 1-D bolt models due to such degrees of freedom being constrained.

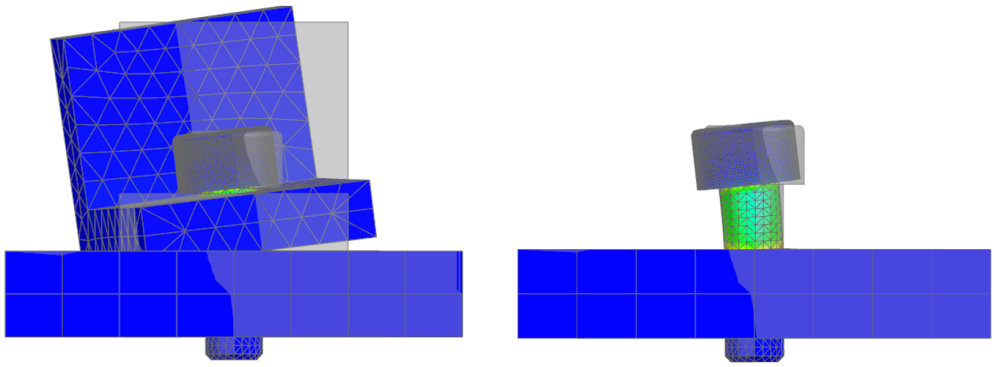

Figure 11. Von Mises stresses in mode 1 (2814 Hz) from case-1

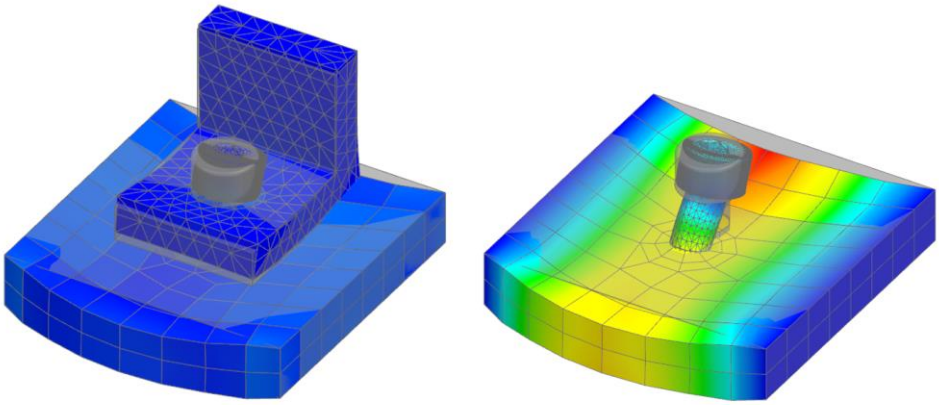

Figure 12. von Mises stresses in mode 12 (35366 Hz) from case-1

Even though the aspect ratio of the overall structure is not particularly high, the detailed model in case-1 is more shows more capability in visualizing the complex motions of the bolt. Where in the simplified models, 1-D bolts' rigidity does not allow as much motion. This increased rigidity in the 1-D elements is the main source is main source of error in the modal frequencies shown in Table 3. Modes that are highly dependent on the motion of the bolts have overestimated frequency values in the simplified models.

4.3 Effect of beam element discreitization

While not steering away from the main objective, the effect of discretizing the 1D beam model of case-3 described in section 3.3.3 was analyzed. More specifically, four subscenarios where investigated, where we discretize the bolt into 2 3, 4 and 10 elements respectively. This was primarily done to try and capture some of the missing mode shapes by offering the beam model more degrees of freedom. The results of the different finite element simulations are summarized in Table 6 below.

Table 6. Effects of varying the number of beam element (case-3) on mode frequencies

Modal frequencies for case-3 (beam) for different model discretization									
mode #	1 element frequency (Hz)	2 elements frequency (Hz)	%	3 elements frequency (Hz)	%	4 elements frequency (Hz)	%	10 elements frequency (Hz)	%
1	NA	NA		NA		NA		NA	
2	2,334	2,335	0%	2,335	0%	2,335	0%	2,335	0%
3	4,772	4,775	0%	4,776	0%	4,776	0%	4,776	0%
4	9,641	9,646	0%	9,647	0%	9,647	0%	9,647	0%
5	13,467	13,033	1%	13,045	1%	13,049	1%	13,054	1%
6	14,720	14,719	0%	14,719	0%	14,719	0%	14,718	0%
7	NA	NA		NA		NA		NA	
8	22,895	22,898	0%	22,898	0%	22,898	0%	22,898	0%
9	23,952	23,952	0%	23,952	0%	23,952	0%	23,952	0%
10	NA	NA		NA		NA		NA	

The % difference shown is calculated with respect to the 1 element showing almost no change in the different mode frequencies. Moreover, no extra mode shapes have been made available by discretizing the bolt into multiple elements. This is because those are torsional mode shapes, and the relevant theta degree of freedom will still be missing regardless of the number of beam elements present in the model.

4.4 System strength evaluation (Static)

Stress values and reaction forces (lateral and axial) in each case/subcase were extracted from the analysis to calculate the margin of safety for the yield, ultimate, slipping and gapping criteria based on Equations 1,2, 4 and 5 respectively. Figure 13 tabulates all MoS calculations for the three simplified finite element models with respect to the full 3D one of case-1. While stress contour plots on the simplified finite element models of cases 2, 3 and 4 are not all that informative, the Von Mises stress are shown here in Figure 13.

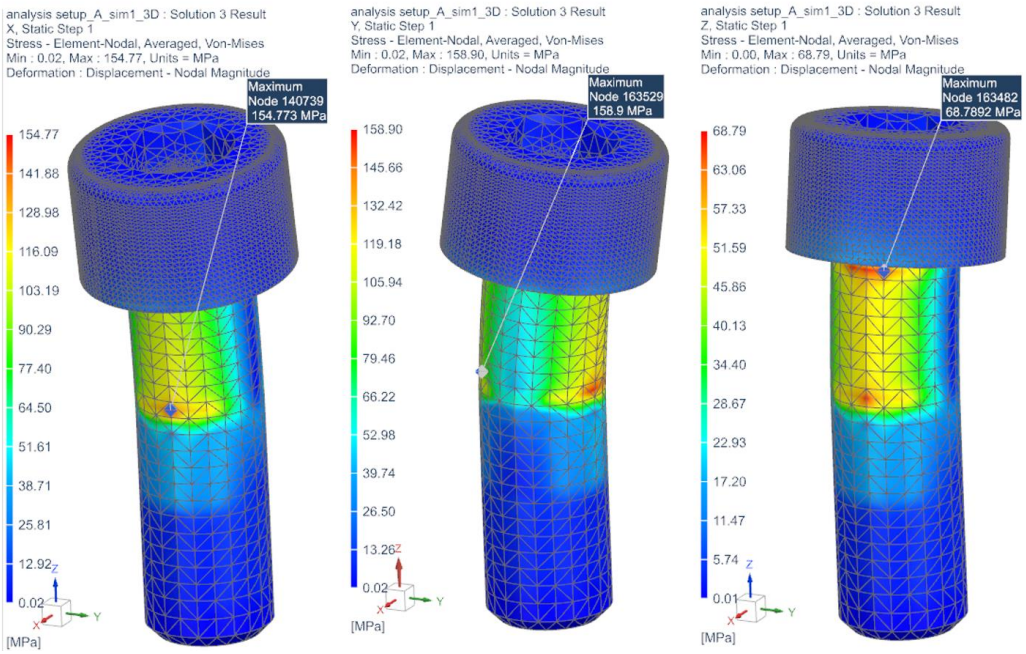

Figure 13. Contour plots of the Von Mises stresses on the three loading scenarios on case-1

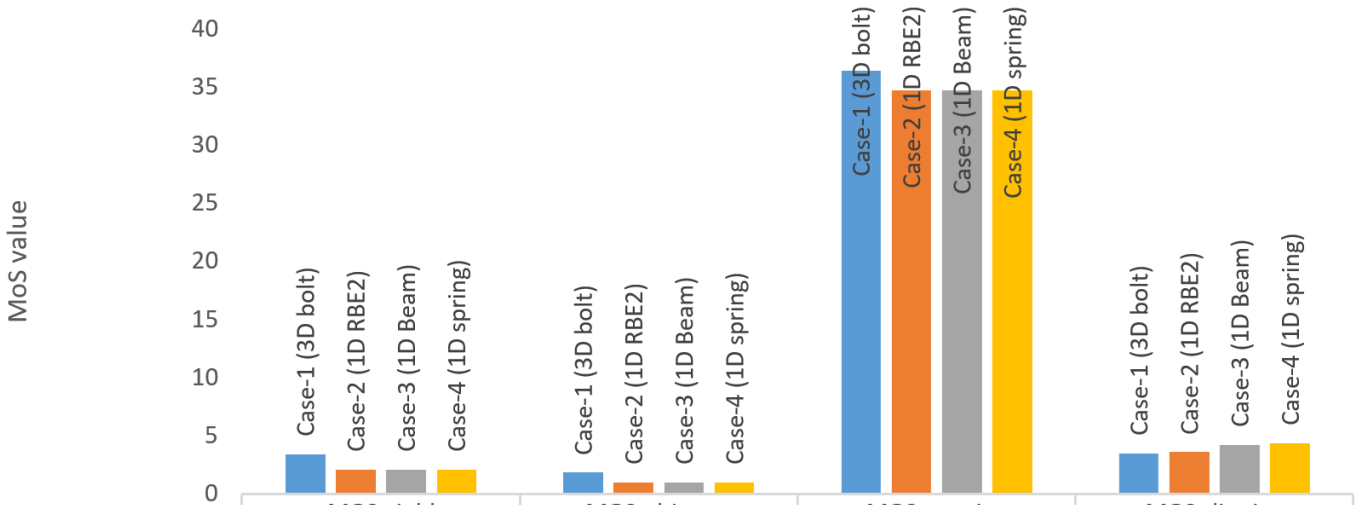

	MOS yield	MOS ultimate	MOS gapping	MOS slipping
Case-1 (3D bolt)	3.41	1.83	36.45	3.51
Case-2 (1D RBE2)	2.11	1.01	34.73	3.61
Case-3 (1D Beam)	2.11	1.01	34.73	4.23
Case-4 (1D spring)	2.11	1.01	34.73	4.36

Figure 14. Bolts' yield, ultimate, gapping, and slipping MoS values for all 4 FEM cases

The results in Figure 14 are based on the most conservative MoS value found in each case/subcase loading scenario. It can be seen that for the yield, ultimate, and gapping MoS, the simplified models show a similar more and slightly more conservative value compared to the detailed model in case-1. The only discrepancy found was in the case of $MoS_{slipping}$ where case-3 and case-4 showed a higher MoS value.

4.5 Bolt size effect

To further expand and validate the results of the different FE simplification modeled used, two more bolts (different sizes and subsequently bolt preloads and tightening torques) were analyzed. The three bolts are the M3, M4 and M5 standardized bolts are summarized in Table 7.

Table 7. Bolt size variations specs [37]

Bolt Data	**M3**	**M4**	**M5**
Nominal Diameter (mm)	3	4	5
Thread pitch, p (mm)	0.5	0.7	0.8
Nominal friction coefficient, $\mu_{threads}$	0.3	0.3	0.3
Bolt friction uncertainty	0.1	0.1	0.1
tightening torque (Nm)	1.1	2.6	5.1
Joint preload (N)	1,135	2,009	3,164

A similar analysis to that presented in section 1.7 was performed on the three bolts with the emphasis placed on the yield criteria, MOS_{yield}. The percentage error for each simplified finite element case for all 3 boll sizes were compared against their respective converged full 3D finite element model. The loading in all bolt simulations was a 50 N

axial load with the same joint configuration and load application location as shown in Figure 7. Only differences are the bolt nominal diameter, thread pitch and the joint pre-load used for each as per the standard [37]. Also, worth noting that the tabulated % error is calculated with respect to the near exact 3D results upon performing a convergence analysis for each of the 3 bolts.

Table 8. Bolt specifications [37]

	M3		**M4**		**M5**	
	MOS_{yield}	% error	MOS_{yield}	% error	MOS_{yield}	% error
Case-1 (3D bolt)	2.04		2.05		2.05	
Case-2 (1D RBE2)	2.04	0	2.05	0	2.11	2.92
Case-3 (1D Beam)	2.03	0.49	2.03	0.97	2.1	2.43
Case-4 (1D spring)	2.03	0.49	2.03	0.97	2.1	2.439

The error is observed to increase with increasing bolt size, while still within acceptable range. For larger assemblies with multiple bolts (granted their stress fields do not interact), it is worth reducing the bolt to a 1D beam model as the computational cost would be higher. In such cases, it is recommended that the factor of safety used in calculating the MOS_{yield} of Equation (4) to be increased to such that the overall output is more conservative. This is in line with what is expected since the larger the bolt size, the lesser of a beam-like behavior it will have, with shear and through-thickness stresses becoming more prevalent.

4.6 Computational time

For this study, all simulation solvers were set to achieve an iterative solver convergence value less than $\mathbf{1 \times 10^{-6}}$. The device used for running the simulations has an Intel Xeon 4-cors processor 32-GB RAM and 64-bit operating system. Taking that into consideration, Table 9 shows the number of nodes and elements in each case and the corresponding analysis computational time. Note that the discretization of case-3 into multiple beam elements detailed section 4.3 did not yield to any tangible increase in the computational time, and are this omitted from Table 9.

Table 9. Computational cost comparison

Case ID	**# of Nodes**	**# of Elements**	**Modal analysis**	**Static analysis**
Case-1 (3D bolt)	114,340	81,201	2min 1sec	1min 45sec
Case-2 (RBE2)	378	326	1 sec	1 sec
Case-3 (1D Beam)	378	326	1 sec	1 sec
Case-4 (1D Spring)	378	326	1 sec	1 sec

5. Conclusion

In summary, the finite element simplification of a standard bolted joint configuration is investigated using Siemens NX software. Static and modal analysis were used to get insight on the accuracy of the simplification by comparing the computational results against a near exact solution of the full 3D finite element model. Both static and modal analysis were performed, and margin of safety values were computed for bolt slipping and bolt gapping phenomena. It can be concluded that simplifying the finite element modeling of bolted joints will yield comparable results while significantly cutting down on computational cost. This is especially the case for smaller bolts (e.g. M3 and M4) where the yield margin of safety was off by less than 1% in comparison with the 3D model. Therefore, it is recommended to maintain a bolt slenderness ratio that is greater than 1.5. While the three simplified models presented here fall short on capturing torsional mode shapes and frequencies, the more common modes and stress results related to the overall behavior of the joint are well captured. It was also determined that further discretizing the 1D model beyond one beam element did not yield any significant improvement in the modal frequencies determined. Moreover, and looking into the four margin of safety criteria used in this manuscript, the three simplified finite element models proved to be more conservative while offering significant savings computational time. This is critical in models with numerous bolted connections, where such finite element simplification will yield a significant reduction in computational costs without sacrificing accuracy.

Author Contributions:

- Conceptualization, A.M. Ibrahim and W.A. Samad.
- Methodology, A.M. Ibrahim.
- Software, A.M. Ibrahim.
- Validation, A.M. Ibrahim and W.A. Samad.
- Investigation, A.M. Ibrahim and W.A. Samad
- Writing—original draft preparation, A.M. Ibrahim.
- Writing—review and editing, A.M. Ibrahim and W.A Samad.
- Supervision, W.A. Samad.

All authors have read and agreed to the published version of the manuscript.

Funding: This research received no external funding

Informed Consent Statement: Not applicable

Acknowledgments: The authors wish to thank the United Arab Emirates' Ministry of Education for their grant that allowed for the acquisition and use of Siemens NX software.

Conflicts of Interest: The authors declare no conflict of interest.

References

[1] A. Khaja, A. Kaliyanda, W. A. Samad and R. E. Rowlands, "Thermoelastic stress analysis of a mechanical fastener," in *Imaging Methods for Novel Materials and Challenging Applications, Volume 3. Conference Proceedings of the Society for Experimental Mechanics Series*, New York, 2013.
https://doi.org/10.1007/978-1-4614-4235-6_14

[2] J. Reid and N. Hiser, "Detailed modeling of bolted joints with slippage," *Finite Elements in Analysis and Design*, vol. 41, no. 6, pp. 547-562, 2005.

https://doi.org/10.1016/j.finel.2004.10.001

[3] F. Esmaeili, M. Zehsaz and T. Chakherlou, "Investigation the effect of tightening torque on the fatigue strength of double lap simple bolted and hybrid (bolted–bonded) joints using volumetric method," *Materials & Design,* vol. 63, pp. 349-359, 2014.
https://dx.doi.org/10.1016/j.matdes.2014.06.021

[4] F. Sen, M. Pakdil, O. Sayman and S. Benli, "Experimental failure analysis of mechanically fastened joints with clearance in composite laminates under preload," *Materials & Design,* vol. 29, no. 6, pp. 1159-1169, 2008.
https://doi.org/10.1016/j.matdes.2007.05.009

[5] G. Valtinat, I. Hadrych and H. Huhn, "Strengthening of riveted and bolted steel constructions under fatigue loading by preloaded fasteners-experimental and theoretical investigations," in *Connections in Steel Structures IV*, 2000.

[6] F. Esmaeili, T. N. Chakherlou, M. Zahsaz and S. Hasanifard, "Investigating the effect of clamping force on the fatigue life of bolted plates using volumetric approach," *Journal of Mechanical Science and Technology,* vol. 27, pp. 3657-3664, 2013.
https://doi.org/10.1007/s12206-013-0911-3

[7] W. A. Samad, A. A. Khaja, A. R. Kaliyanda and R. E. Rowlands, "Hybrid Thermoelastic Stress Analysis of a Pinned Joint," *Experimental Mechanics,* vol. 24, pp. 515-525, 2014.
https://doi.org/10.1007/s11340-013-9822-6

[8] A. I. o. S. C. (AISC), " Manual of steel construction, load and resistance factor," 1986.

[9] M. A. McCarthy, V. P. Lawlor and W. F. Stanley, "An Experimental Study of Bolt-Hole Clearance Effects in Single-lap, Multibolt Composite Joints," *Journal of Composite Materials,* vol. 39, no. 9, pp. 799-825, 2005.
https://doi.org/10.1177/0021998305048157

[10] M. M. Frocht and H. N. Hill, "Stress concentration factors around a central circular hole in a plate loaded through a pin in the hole," *Applied Mechanics,* vol. 7, pp. 5-9, 1940.

[11] A. A. Khaja and W. A. Samad, "Hybrid Digital Image Correlation," Journal of Engineering Mechanics, vol. 146, no. 4, 2020.

[12] W. Wunderlich and W. Pilkey, "Mechanics of Structures. Variational and Computational Methods," *Meccanica,* vol. 39, pp. 291-292, 2004.

[13] R. Grzejda, "Modelling bolted joints using a simplified bolt model," *Journal if Mechanical and Trasport engineering,* 2017.
DOI 10.21008/j.2449-920X.2017.69.1.03

[14] E. Paroissien, F. Lachaud, S. Schwartz, A. Da Veiga and P. Barriere, "Simplified stress analysis of hybrid (bolted/bonded) joints," *International Journal of Adhesion and Adhesives,* vol. 77, pp. 183-197, 2017.
10.1016/j.ijadhadh.2017.05.003

[15] K. J. Belisle, "Experimental and Finite Element Analysis of a Simplified Aircraft Wheel Bolted Joint Model," The Ohio State University, Ohio, 2009.

[16] J. G. Williams, R. E. Anley, D. H. Nash and T. G. Gray, "Analysis of externally loaded bolted joints: Analytical, computational and experimental study," *International Journal of Pressure Vessels and Piping,* vol. 86, no. 7, pp. 420-427, 2009.
https://doi.org/10.1016/j.ijpvp.2009.01.006

[17] J. Montgomery, "Methods for Modeling Bolts in the Bolted Joint," in *ANSYS User's Conference Vol 5*, Orlando, FL, 2002.

[18] J. Kim, J.-C. Yoon and B.-S. Kang, "Finite element analysis and modeling of structure with bolted joints," *Applied Mathematical Modelling,* vol. 31, no. 5, pp. 895-911, 2007.
https://doi.org/10.1016/j.apm.2006.03.020

[19] B. Reuss, Computer Aided Technology, LLC, 2018. [Online]. Available: https://www.cati.com/blog/2018/11/why-you-should-simplify-your-analysis/

[20] W. A. Samad and K. Suresh, "CAD-integrated analysis of 3-D beams: a surface-integration approach," *Engineering with Computers,* vol. 27, no. 3, pp. 201-210, 2011.

[21] L. Paracchini, C. Barbieri, M. Redaelli, D. Di Croce, C. Vincenzi, and R. Guarnieri, "Finite Element Analysis of a New Dental Implant Design Optimized for the Desirable Stress Distribution in the Surrounding Bone Region," *Prosthesis,* vol. 2 , no. 3, pp. 225-236, 2020.

[22] M. Cicciù, G. Cervino, D. Milone, and G. Risitano, "FEM Investigation of the Stress Distribution over Mandibular Bone Due to Screwed Overdenture Positioned on Dental Implants," *Materials*, vol. 11 , no. 9, pp. 1512, 2018.

[23] H. Relf, C. Barberio, and D. Espino, "A Finite Element Model for Trigger Finger," *Prosthesis*, vol. 2, pp. 168-184, 2020.

[24] J. S. Tsai and Y. F. Chou, "The identification of dynamic characteristics of a single bolt joint," *Journal of Sound and Vibration,* vol. 125, no. 3, pp. 487-502, 1988.
https://doi.org/10.1016/0022-460X(88)90256-8

[25] A. Javanmardi, R. Abadi, A. Marsono, M. T. Masine, I. Zulkepli and A. Ahmad, "Correlation of Stiffness and Natural Frequency of Precast Frame System," *Applied Mechanics and Materials,* vol. 735, pp. 141-144, 2015.
https://doi.org/10.4028/www.scientific.net/AMM.735.141

[26] "Slippage in bolted connections," EnterFEA, 2016.

[27] Andy, "Bolts, Preload Explained," 29 December 2017. [Online]. Available: https://medium.com/@bananajutsu/bolted-joint-preload-9ead1f81511b.

[28] R. Wingate, *An overview of Fastener Requirements in the new NASA-STD-5020,* NESC Academy NASA, 2013.

[29] D. Derry, "Rules of Thumb for Thread Engagement," Field Fastener, 13 March 2018. [Online]. Available: https://fieldfastener.com/2018/03/13/rules-of-thumb-for-thread-engagement/.

[30] Genfast, "Minimum Thread Engagement (Bolt Failure) Chart - Metric," General Fastener Comany, Madison Heights, MI.

[31] S. Ghosh, "Screw or Bolt Thread Engagement Length Calculation," MechGuru , 7 December 2012. [Online]. Available: https://mechguru.com/machine-design/screw-or-bolt-thread-engagement-length-calculation/.

[32] J. D. Reid and N. R. Hiser, "Detailed modeling of bolted joints with slippage," *Finite Elements in Analysis and Design,* vol. 41, no. 6, pp. 547-562, 2005.

[33] E. C. f. S. Standardization, "Threaded fasteners handbook," Noordwijk, 2010.

[34] K. H. Brown, C. Morrow, S. Durbin and A. Baca, "Guideline for Bolted Joint Design and Analysis: Version 1.0," Sandia National Laboratories, Albuquerque, 2008.

[35] P. Esnault and M. Klein, "Factors of safety and reliability—present guidelines & future ts," Proceedings of the conference on spacecraft structures, materials & mechanical testing, SP-386, Nordwijk, The Netherlands, March 27–29, European Space Agency, pp. 109–119, 1996

[36] K. Bernstein, R. Kujala, V. Fogt and P. Romine, "Structural Design Requirements and Factors of Safety for Spaceflight Hardware: For Human Spaceflight," National Aeronautics and Space Administration Lyndon B. Johnson Space Center, Houston , 2011

[37] Bossard, "Hex socket head cap screws," Bossard, [Online]. Available: https://eu.shop.bossard.com/group/en/8500/socket-products/hex-socket-head-cap-screws/bn-7_hex-socket-head-cap-screws-fully-threaded.